Application of remotely sensed data integrating with DEM for deriving surface reflectance and global albedo in Heihe River basin, Northwestern China

LIU Sanchao, ZHANG Wanchang

International Institute for Earth System Science, Nanjing University

Abstract: Traditional atmospheric correction methods are complicated in theory, difficult in practice owing to some parameters, especially field real-time atmospheric profile data, are seldom available. This study presents an easy, fast approach that takes the best use of DEM in association with the application of an atmospheric correction model to obtain the surface reflectance from Landsat TM images over the Heihe river basin. Based on surface reflectance imaginaries for TM Band1-5 and 7, different band integration approaches are attempted to obtain the total continuous spectral albedo over the study site for comparing with the field observed ones. It was found that for vegetated area the TM band 2, 4, 7 integrating approach performs better, while for non-vegetation area band integration using TM1-5 and 7 is more reliable.

1 Introduction

Land surface reflectance and global albedo are very important parameters in meteorological, agricultural and hydrological research, and they are the key factors on studying the interaction in land surface-atmosphere-sensor system. Traditional atmospheric correction methods are very complicated in theory and need some simultaneous atmospheric profile data that are often hard to obtain; other methods are based on dark target theory but unfortunately the results usually are not satisfying. Due to these reasons, to seek a convenient and reliable atmospheric correction method becomes difficult and urgent for remotely sensed science.

Because remotely sensed data are discontinuous spectral images, the global albedo of entire continuous spectral of VSWIR (from VNIR to MIR) bands should be integrated by different bands. One method is to make land cover classification firstly and albedo is obtained using TM band2,4,7, such as Brest et al. using MSS 4,7 bands and Duguay et al. using TM2,4,7[1,2]; another method is to integrate 6 TM bands from visible to MIR spectral [3,4].

In this paper, we use an easy and convenient method to make atmospheric correction which is put forward by Gilabert[5,6]. Based on land surface reflectance imaginaries for TM Band1-5 and 7, two methods of deriving global albedo are compared and the different results are calibrated with field data. The best integrated bands on derivation of surface global albedo in HEIXI corridor of HEIHE river basin was showed in the article.

2 Study area and data

The study area covers an area about 9000km^2 and mainly lies in mid-up Heihe river basin that is a very important inland basin in northwestern China (figure 1.). In this area, Zhangye city and Zhangye oasis and a part of Qilian Mountain are included and the annual mean precipitation is 140mm and annual mean air temperature is about 7℃ in the entire region. For lying in oasis transition zone, land use and land cover

vary greatly seasonally.

Figure 1. The sketch map of Heihe river basin

The data used in this research are mainly included digital elevation model (DEM) and Landsat TM images. DEM covers an area about 9000 km^2 and its spatial resolution is 30m*30m. Remotely sensed images are Landsat-4 thematic mapper. In order to consistent with DEM's spatial resolution for making topographic correction, TM images of bands 1-5,7 are resized into 30m*30m.The images are made geometric correction using 12 GCPS points and maximum error is less than 0.5 pixel.

3 Theory and methods

3.1 Topographic correction

Terrain affects the land surface energy distribution and the satellite sensor acceptant information greatly, especially in rugged mountain to relief topographic influence is indispensable [7]. Topographic correction for TM images using high resolution DEM can improve the precision of the surface reflectance which are calculated by atmospheric correction [6]. Since the study mostly lies in the middle of Hexi corridor, the land surface terrain variety is not too much in most study area and the vegetation mainly covers in the north slope of the mountain area around Zhangye, only the first stage normalization to relief shadow effect for RS images is used in this study [7].

Firstly, the solar elevation and azimuth angle can be easily found in the head file of the TM data so that the shade relief model can be set up to simulate the distribution of terrain shadow. The method need integrate the geometric correction TM images with the same spatial resolution DEM and every band's reflectance are calculated according to the following formula :

$$\delta DN_{\lambda ij} = DN_{\lambda ij} + DN_{\lambda ij} * (\mu_k - X_{ij}) / \mu_k \qquad (1)$$

Where dDN_{ij} stands for the normalized radiance data, DN_{ij} for the raw radiance data for pixel ij in band ; μ_k is the mean value for entire scaled [0,255] illumination model and X_{ij} the scaled [0,255] illumination value. The comparison result between before and after topographic correction is shown in table 1.

Table 1. Comparison of the mean DN values for forest and bare ground before and after topographic correction

TM Band	Forest				Bare soil			
	Before correction		After correction		Before correction		After correction	
	Northern aspect	Southern aspect	Northern aspect	Southern aspect	Northern aspect	Southern aspect	Northern aspect	Southern aspect
1	151.1	106 5	139	114.6	178	124.3	146.6	134 2
2	71.2	49.3	61.4	53.6	79.1	58.8	69.5	63.1
3	78 9	63.1	72.4	68.9	127	76.5	96.2	86.2
4	130.2	89 8	122.8	102.3	104	65	85.2	76.2
5	170.5	150.3	162.5	156.3	208	140.2	192	163 3
7	89.6	79.1	83.4	82.1	138	77.5	122.5	102.4

3.2 Atmospheric correction

The purpose of atmospheric correction is to obtain real reflectance of land surface target. There are many atmospheric correction methods but few are based on TM images directly. Gilabert and Zhang put forward an easy and convenient atmospheric correction method [5,6]. The model is based on three assumptions: (1) the earth's surface is Lambertian in nature; (2) in the darkest pixels of TM 1,3,there is only the atmosphere contribution radiance and the land surface reflectance is close to zero; (3) the multiple scattering in the atmosphere and the adjacent pixel effect are neglected.

Based on topographic correction and the above assumptions, the sensor received radiance can be calculated by taking use of TM data head file firstly; then the dark pixel can be found in the cloud shadow of the image and the DN value of band 1 and band 3 can be also gained. Based on the result some atmosphere parameters can be inferred; on the base of dark pixel of band 1 and 3 all bands' atmosphere radiation can be calculated; then the total energy received by the surface target should be obtained; at last, the relationship between land surface reflectance and the DN value of 6 TM bands after topographic correction can be set up.

3.2.1 Land surface reflectance, Rs[Q]

Since the natural surface is assumed Lambertian, land surface reflectance can be calculated according to the following formula :

$$R_s[\lambda] = (K * (L_0[\lambda] - L_p[\lambda])) / (E_g[\lambda] * T_u(\lambda) * \cos\theta_0 \qquad (2)$$

Where is the central band length of different TM bands, K is the distance between the sun and the earth while the satellite was overpassing the study site, θ_0 is solar zenith angle. $L_0[\ ]$ is the radiance received by sensor, $L_p[\ ]$ is the atmospheric radiance, $E_g[\ ]$ is the total radiance of the surface , T ↑ ( ) is the upward atmosphere transmittance .

3.2.2 Sensor received radiance, $L_0[y]$

The radiance of Landsat-4 TM sensor has the following linear relationship with DN:

$$L_0[\lambda] = A_1 * DN[\lambda] + A_0 \quad (3)$$

Where $L_0[\ ]$ is the radiance received by sensor, A_1 and A_0 are the calibration coefficient of different bands and equal to the gains and offset in TM data head file.

3.2.3 Atmospheric radiance, $L_p[\ ]$

In Gilabert's model, atmospheric radiance includes Rayleigh ($L_r[\ ]$) and aerosol ($L_a[\ ]$) contribution radiance:

$$L_p[\lambda] = L_r[\lambda] + L_a[\lambda] \quad (4)$$

In this model, the dark pixel should be carefully found in the cloud's or mountain's shadow in the TM images after topographic correction. For the dark pixel, satellite sensor only receive the atmosphere contribution radiance but not the land surface contribution radiance[8] :

$$L_0^*[\lambda] \approx L_p^*[\lambda] \quad (5)$$

Where * refers to the selected dark pixel.

As for Rayleigh radiance, the optical thickness for the ozone τ oz(λ) should be obtained by taking use of interpolation method[9] firstly and the molecular optical thickness τ r(λ,h) can also be obtained according to the average elevation in Zhangye oasis, the Lr*[λ] of TM-1 and TM-3 can be calculated according to Saunders,1990[10]. Aerosol contribution radiance (L_a*[ ]) can be calculated according to formulae 3-5.

Once $L_p[1]$ and $L_p[3]$ have been computed from the dark pixel, it is possible to calculate atmosphere radiance of other bands. Rayleigh contribution, $L_r[\ ]$ is practically constant in the atmosphere and only dependant on the solar and view zenith angles (in this paper, =0). So it can be evaluated according to Saunder's method, too.

As for aerosol contribution radiance, it has the following relationship to band length :

$$L_a[\lambda] = \Gamma \lambda^{-\delta} \quad (6)$$

G, d are two basic parameters of concentration and size distribution of aerosol particles. With two La*[ ] of band1 and band3, *G, d* can be calculated by two formulae. Other bands' aerosol contribution radiance are easy to be calculated according (6) because we have obtained *G, d.*

The other parameters, such as aerosol optical thickness ta( ), upward and downward atmosphere transmittance T ( )、T ( ) et al., can be calculated according to Gilabert because our study area lies in the inter continent region.

3.2.4 Global solar irradiance, $E_g(\ )$

Since multiple scattering in the atmosphere and the effect of adjacent target are neglected, the global solar irradiance is the sum of direct irradiance ($E_b[\ ]$) and diffuse irradiance ($E_d[\ ]$). The two important parameters are also calculated according to Gilabert's paper[5].

Based on the above work, land surface reflectance of band1-5 and 7 can be obtained according to formula 2. Some important atmosphere parameters of our image are shown in table 2.

Table 2. Some important parameters obtained in the process of atmospheric correction

Solar Zenith Angle	Cos($_0$)	Pr	Hr(ho)	d	G	Pa
27.69	0 8855	1.338	0.8346	3.3631	1.9457	2.132
	TM1	TM2	TM3	TM4	TM5	TM7
Eo( )	620	577	493	332	67.1	24.5
r(,ho)	0.1421	0.0703	0.0388	0.0154	0.0009	0.0003
toz( )	0.009	0.156	0 226	0.101	0.325	0.112
Lo( )	32.216		9.305			
Lr( )	7.94	2 878	1.207	0.431	0.003	0.0006
DN*	56		13			
La*( )	24.2762		8.0979			
Lp*( )	32.2162		9.3049			
ta( )	0.276	0.192	0.147	0.072	0.05	0.033
T ( )	0.858	0.796	0 766	0.889	0.722	0.894
T ( )	0.799	0.738	0.712	0.851	0.678	0.872
Lp( )	32 216	16.302	9.305	4.105	0.333	0.126
Eb( )	438.591	377.21	311.057	250.036	40.269	18.913
Ed( )	98.302	91 923	79.656	30.143	11.242	2.011
Eg( )	536.893	469.132	390.714	280.178	51.511	20.923
Rs(min)	0.0047	0.0062	0.0059	0.0117	0.0083	0.0004
Rs(max)	0.3092	0.8536	0.7198	0.8122	0.8202	0.8658

At last, the relationship between reflectance and DN value of TM band1-5 and 7 can be obtained as following:

$$R_s[1] = 0.0015776 * DN[1] - 0.088361 \quad (7)$$

$$R_s[2] = 0.0360623 * DN[2] - 0.058751 \quad (8)$$

$$R_s[3] = 0.0030124 * DN[3] - 0.039296 \quad (9)$$

$$R_s[4] = 0.0037464 * DN[4] - 0.025813 \quad (10)$$

$$R_s[5] = 0.0033274 * DN[5] - 0.021666 \quad (11)$$

$$R_s[7] = 0.0034889 * DN[7] - 0.016912 \quad (12)$$

Where Rs[i] (i=1-5,7) is the land surface reflectance of band i, DN[i] (i=1-5,7) is the DN value of band i after topographic correction

3.3 Determination of the land surface global albedo, a

There are many methods to calculate continuous spectral region albedo from visible to mid-infrared

discrete TM bands[1,2,3,4]. When albedo is calculated with band2,4,7 for driving it should make rough land use and land cover classification because the numbers of used band are relatively few , while with 6 bands images albedo can be calculated by reflectance data directly because the spectral region is relatively continuous and wide .

3.3.1 Determination of global albedo using TM 2,4,7

Under different atmospheric conditions, solar energy distributes differently in total continuous spectra range. Because the sky is clear and cloudless when the satellite was overpassing the study area, NASA's[11] result may be applied to our study[11]. In this method, another important factor is land use classification. Tucker put an easy method that land cover can be roughly classified into vegetation area and non-vegetation area [12].

For the reflectance of vegetation is low in visible band and high in infrared band and relatively midst in mid-infrared band, TM2、TM4 and TM7 can correspond to the three spectral ranges and are endowed with the following weights to calculate global albedo:

$$\alpha = 0.526R_s[2] + 0.362R_s[4] + 0.112R_s[7] \tag{13}$$

The spectral character of non-vegetation area is simple and can be divide into visible band（0.3 ~ 0.725μm）and mid-infrared band(0.725 ~ 4.0μm) spectral range. The global albedo in non-vegetation area can be derived as following formula :

$$\alpha = 0.526R_s[2] + 0.474R_s[4] \tag{14}$$

3.3.2 Determination of global albedo using TM 1-5,7

TM images have 7 useful bands. In order to use the different bands sufficiently, 6 bands except TM6 can be integrated to calculate global albedo. With the continuous spectral range from 0.3μm to 4μm, three water absorption windows of 1.38-1.50μm,1.85-2.08μm,2.35-3.00μm are neglected[13,14]. The land surface global albedo is integrated by use of the method presented by Dubayah and Wang[3,4].

$$\alpha = 0.221R_s[1] + 0.162R_s[2] + 0.102R_s[3] + 0.354R_s[4] + 0.068_s[4] + 0.059R_s[5] + 0.0195R_s[7] \tag{15}$$

4 Result and discussion

In this paper, in order to derive surface global albedo two methods are used and compared. The result using band2,4,7 is showed in figure 2. The mean albedo is 0.2780 for total study area and the mean value of vegetation area is 0.2114 while 0.2881 of non-vegetation area. In this figure, the low value region is main water body and shadow of cloud, and high value region is bare soil and desert of non-vegetation and middle region is vegetation area.

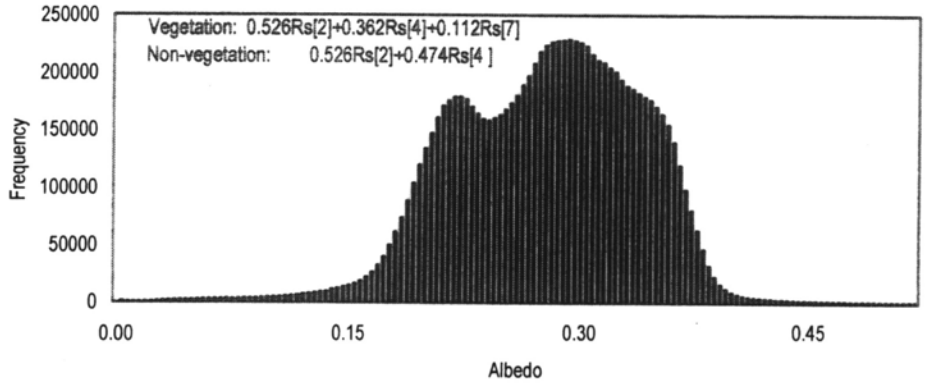

Figure2. Albedo Histogram obtained by reflectance integration with bands 2,4,7

Figue 3 is the albedo histogram for the entire study area by integrating of TM1-5 and 7. The mean albedo is 0.2879 for total study area, and there are two evident value ranges: one is from 0.1640 to 0.2626 which represents vegetation area and the other range is from 0.2626 to 0.4105 which represents non-vegetation area .

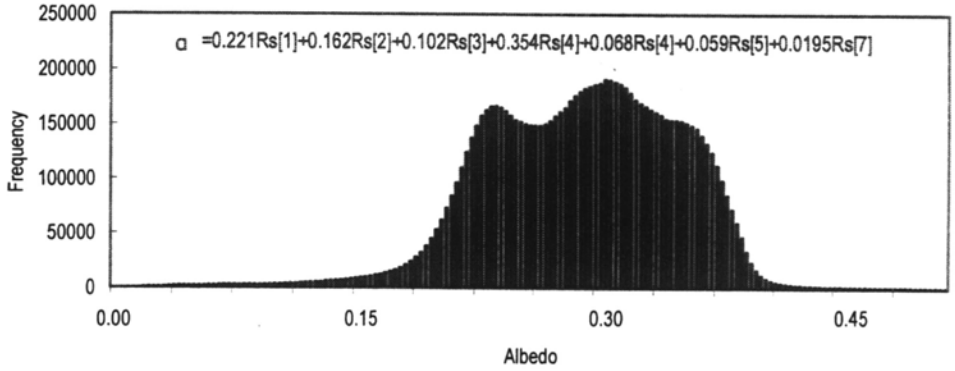

Figure 3. Albedo histogram obtained by reflectance integration with bands 1-5,7

As shown in above two figures, the two histograms have the same pattern that they have two evident value ranges that one is main vegetation and another is non-vegetation area. In order to compare the two results further, table 3 shows some typical land covers' global albedo that are obtained by the two different approaches.

Table 3. Comparison of albedo obtained for some land covers with two different approaches

Land cover	Albedo					
	(band 2,4,7)			u (band 1-5,7)		
	Min	Max	Mean	Min	Max	Mean
Oasis farmland	0.145	0.275	0.205	0.158	0.279	0 227
Urban and residential area	0.103	0.315	0.217	0 108	0.310	0 222
Water body	0.026	0.176	0.058	0.023	0.171	0 048
Bare soil	0.253	0.418	0 316	0 267	0.427	0.329
Forest (moutain)	0.092	0.364	0 212	0.099	0.395	0.223

On the basis of long time field observation, table 4 shows the result of the comparison between measured in field data and estimated in above two approaches for several typical land covers' monthly mean albedo over Heihe River Basin in June.

Table 4. Comparison of the mean albedo measured and estimated for several typical land covers in June over Heihe River Basin

Land use	Measured	Estimated	
		U (band 2,4,7)	u (band 1-5,7)
Grassland + forest	0.1896	0.2117	0.2275
Farmland *	0 1896	0.2048	0.2268
Bare land	0.3672	0.3164	0.3268
Urban and residential area	0.2253	0.2166	0.2218

* : monthlymean value of farmland equal to the value of Grassland + forest

As shown in table 4, for vegetation area the result using model is better than model and the error is close to 9%, while in non-vegetation area model 's result is more close to measured data and the error is about 10%. So in this article to calculate global albedo by means of the reflectance of TM bands, we use model in vegetation area and model in non-vegetation area. The result is shown in figure 4.

Figure 4. The image of albedo generated with the band integration method presented in the context
(subset image of albedo with 2110*1794 pixels around Zhangye)

5 Concluding remarks

The pre-processing of remotely sensed data is very important for remote sensing science. By integrating TM images and digital elevation model (DEM) the topographic correction is presented and the correction result is discussed. Based on this work, an easy and fast approach of an atmospheric correction model to obtain the surface reflectance from Landsat TM images over the Heihe river basin is also applied. Based on surface reflectance imaginaries for TM Band1-5 and 7, different band integration approaches were attempted to obtain the total continuous spectral albedo over the study site for comparing with the field observed ones. It was found that the best band integration approaches in Heihe

river basin for different types of land use and land cover. In the future works, different temporal and spatial resolution satellite data such as NOAA AVHRR, Landsat-7 ETM+, MODES et al., should be calibrated and applied to derive the land surface parameters such as land surface reflectance, global albedo, heat flux and evopotranspiration et at. in different study areas and different scales.

References

[1] Brest C L and Goward S N. Deriving surface albedo measurements from narrow satellite data. *International Journal of Remote Sensing*, 1987, 8: 351-367.

[2] Duguay C R. Estimating surface reference and albedo from Landsat-5 Thematic Mapper over rugge terrain. *PE & RS*, 1992 , 58: 551-558.

[3] Dubayah R. Estimating net solar radiation using Landsat Thematic Mapper and digital elevation data . *Water Resource Research*, 1992, 28: 2469-2484.

[4] Wang J, Write K. and Roberson G J. Estimating surface net solar radiation by use of Landsat-5 TM and digital elevation models. *International Journal of Remote sensing*. 2000, 21 (1): 31-43.

[5] Gilabert M A, Conese C. and Maselli F. An atmospheric correction method for the automatic retrieval of surface reflectance from TM images. *INT.J.REMOTE SENSING*, 1994, 15(10): 2065-2086.

[6] Zhang W C, Yamaguchi Y and Ogaw K. Evaluation of the Pre-processing of the Remotely Sensed Data on the Actual Evapotraspiration ,Surface Soil Moisture Mapping by an Approach Using Landsat,DEM and Meteorological Data. *Geocarto Inter*, 2000, 15(4): 57-67.

[7] Civico D L. Topographic normalization of Landsat Thematic Mapper digital imagery. PE & RS, 1989, 55(9): 1303-1309.

[8] Kaufman Y J. The atmospheric effect on remote sensing and its corrections. In Theory and Applications of Optical Remote sensing, edited by G. Asrar (New York: John Wiley & Sons), 1989: 336-428.

[9] Sturm B. The atmospheric correction of remote sensing data and the quantitative determination of suspended matter in marine water surface layers. In Remote Sensing in Meteorology, Oceanography and Hydrology, Edited by A. P. Crachnell (Chichester: Ellis Horwood Limited), 1981, chapter 11.

[10] Saunders R W. The determination of broad band surface from AVHRR visible and near-infrared radiances. *International Journal of Remote sensing*, 1990, 11: 49-67.

[11] NASA, 1974. Surface atmospheric extremes (launch and transportation areas). National Aeronautics and space Administration Document SP-8084, revised June.

[12] Tucker C J. Red and photographic infrared linear combination for monitoring vegetation. *Remote Sensing of Environment*, 1979, 8:127.

[13] Irons J R, and Ranson K J. Estimating big bluestem albedo from directional reflectance measurements. *Remote sensing of Environment*, 1988, 25:185-199.

[14] Ranson K J, Irons, J R, and Daughthy C S T. Surface albedo from bi-directional reflectance. *Remote sensing of Environment*, 1991, 35: 201-211.